

ASSESSMENT OF SOIL EROSION RISK USING RUSLE IN SELECTED WATERSHEDS OF SULAIMANI PROVINCE, IRAQ

Star Sadiq Abdullah^{1*} Hussein Asadi², Khalid Tayeb Mohammed Barzinji³ Tariq Hama Karim⁴ Ali Akbar Nazari Samani⁵

² Faculty of Natural Resources, University of Tehran, Karaj, Iran

³ Department of Natural Resources, College of Agricultural Engineering Sciences, University of Sulaimani, Sulaimani, Iraq

⁴ Department of Surveying and Geomatics Engineering, Faculty of Engineering, Tishk International University, Erbil, Iraq.

⁵ Faculty of Natural Resources, University of Tehran, Karaj, Iran

ABSTRACT

This study was aimed to assess the risk of soil erosion in 32 watersheds of Sulaimani province, Kurdistan/Iraq, based on Revised Universal Soil Loss Equation, GIS and RS data. The annual precipitation data were used to generate the rainfall-runoff erosivity factor using the previously developed equation for the region. The soil erodibility factor was estimated using soil particle size distribution data. The topographic factor was generated using a digital elevation model from a sentinel 2. The cover-management factor was determined by using Google Earth Engine with Landsat7 and Landsat8. While the soil erodibility and vegetation factors did not show high spatial variability across the province, rainfall erosivity showed an increasing trend from south west to north east of the region, ranged from 73 to 632 MJ mm ha⁻¹ h⁻¹. The results showed that the average annual soil loss for the different watersheds ranged from 2.12 to 62.05 t ha⁻¹ y⁻¹. The results also indicated that the main factors governing soil erosion in Sulaimani province are rainfall intensity, rugged topography, steep slopes, and sparse vegetation.

Key words: conservation, erodibility, remote sensing, Suleimani, vegetation cover.



Copyright© 2025. The Author (s). Published by College of Agricultural Engineering Sciences, University of Baghdad. This is an open-access article distributed under the term of the Creative Commons Attribution 4.0 International License, which permits unrestricted use, distribution, and reproduction in any medium, provided the original work is properly cite.

Received: 19/8/2023, Accepted: 13/12/2023, Published: 28/02/2026

INTRODUCTION

Accelerated land degradation during the 20th and early 21th centuries (Molnárová, *at el.*,2023) has induced a great threat to both agriculture and environment (i.e. food security, livelihoods sustainability, ecosystem services and biodiversity conservation) (Abdel Rahman, 2023; Molnárová, *at el.*,2023). Land degradation is the result of intensifying and converging pressures for livestock and agricultural production, urbanization, deforestation, and extreme weather events like drought and intense rainfalls (AbdelRahman,2023, 16, 20). Water and wind erosion are the most recognized and dominant types of land degradation (Molnárová, *at*

el.,2023). The problem of desertification is also one of the main challenges that have become a threat at present, as it contributes to the reduction of agricultural lands and their low productivity in areas with arid and semi-arid climatic characteristics. Water erosion negatively impacts the natural, physical, and chemical properties of soils (Mehdizade *et al.*, 2013). Studies on soil and water management (i.e. watershed management) are of vital importance in arid and semi-arid regions for protecting limited natural resources (Sreedevi *et al.*, 2013) and this practice requires information on watershed characteristics. On the other hand, it is not possible to implement rehabilitation programs in all areas at a time

(Sreedevi *et al.*, 2013). For this reason, prioritization plays a major role in the identification of the areas which are in need of immediate action. The most practical and commonly used soil erosion prediction models are USLE and RUSLE, because they need low input data and can be applied simply on the watershed scale (Zhang *et al.*, 2009.). The factors used in these models were usually estimated or calculated from field measurements. The methods of quantifying soil loss based on erosion plots possess many limitations in terms of cost, representativeness, and reliability of the resulting data. They cannot provide spatial distribution of soil erosion loss due to the constraint of limited samples in complex environments. So, mapping soil erosion over large areas is often difficult using these traditional methods (Asadi, *et al.*, 2017). Spatial technologies such as remote sensing (RS) and geographical information system (GIS) techniques have been used for assessment soil erosion and its spatial distribution feasible with reasonable costs and better accuracy in larger areas (e.g. Singh *et al.*, 2023). In general, the land-cover classifications can be obtained from the cover-management factor image by remote-sensing data, while the topographic factor from DEM data, data interpolation of sample plots, and calculation of soil erosion loss are obtained from GIS (Wang *et al.*, 2003). Many researchers have used USLE/RUSLE for mapping soil loss across the watersheds in GIS environment (e.g. Gelagay and Minale, 2016; Asadi *et al.*, 2017; Fallah *et al.*, 2023; Räsänen *et al.*, 2023). Since there are scanty measured data for specified scales (Sreedevi *et al.*, 2013), spatial field-based evaluations of soil erosion and validation of the geographic soil loss projections are achieved by soil erosion models (Prasuhn *et al.*, 2013) are impossible. As a result, the predicted values are called soil erosion risk, and mainly used qualitatively to show only the relative risk in different watersheds or spatial risk in a watershed (i.e. prioritization). Based on the report by Eltaif and Gharaibeh (Eltaif and Gharaibeh, 2022), about 11 M ha of lands suffer from severe water and wind erosion in Iraq. In northern Iraq, an area about 12 M ha are affected by water

erosion. Agricultural expansion and land mismanagement (i.e. deforestation, overgrazing and conventional cultivation) are the main causes of increasing soil erosion in this semiarid region (Keya, 2018). Soil water erosion is high in the mountainous regions of north and northeast with high rainfall intensities (Keya, 2018; Eltaif and Gharaibeh, 2022). Overcoming the problem of soil erosion in the region especially in area with high risk needs a soil conservation planning and management strategies (Abdel Rahman, 2023) which in turn would be based on detail knowledge on the spatial rate of soil erosion and governing forces (Eltaif and Gharaibeh, 2022). Although there are few research works (Keya, 2018) in other regions of north and north-east of Iraq dealing with soil erosion assessment, to the best knowledge of the authors, there are no studies concerning the spatial rate of soil erosion and most affecting factors in Sulaimani province. This study integrates the RUSLE model with RS and GIS techniques to assess the spatial distribution of soil erosion risk and evaluate most important governing factors in Sulaimani province, Iraq.

MATERIALS AND METHODS

Study area: The study area is located the realm of the mountainous area of Iraqi Kurdistan region within Sulaimani province, between longitude ($4^{\circ} 45' 29''$ - $46^{\circ} 20' 25''$) East and latitude ($34^{\circ} 33' 39''$ - $36^{\circ} 29' 15''$) North (Figure 1), with a total area of (2014400 ha). It is bounded to the north and east by Iraqi-Iranian borders, to the west by the Lesser Zab river and to the south by Kirkuk and Diyala governorates. To evaluate the soil erosion risk and the main affecting factors, 32 watersheds of different sizes were randomly selected across the Sulaimani province (Figure 1). Some selected characteristics of the watersheds are presented in Table 1.

The input factors of rusle : Revised Universal Soil Loss Equation (RUSLE) is a well-known, universally accepted and an empirical soil erosion model. The RUSLE was developed based upon six factors—rainfall erosivity factor (R), soil erodibility factor (K), slope length and steepness factors (LS), cover management factor (C) and conservation practice factor (P) for the estimation of the average annual soil loss (A) according to (24):

$$A = R \times K \times LS \times C \times P (1)$$

where A is annual soil loss (tons ha⁻¹ y⁻¹), R is rainfall erosivity (function of total rainfall and rainfall intensity) (MJ mm ha⁻¹ h⁻¹ yr⁻¹), K is

erodibility of the soil (t ha h MJ⁻¹ ha⁻¹ mm⁻¹) (function of soil texture, soil organic matter, soil structure and soil permeability),

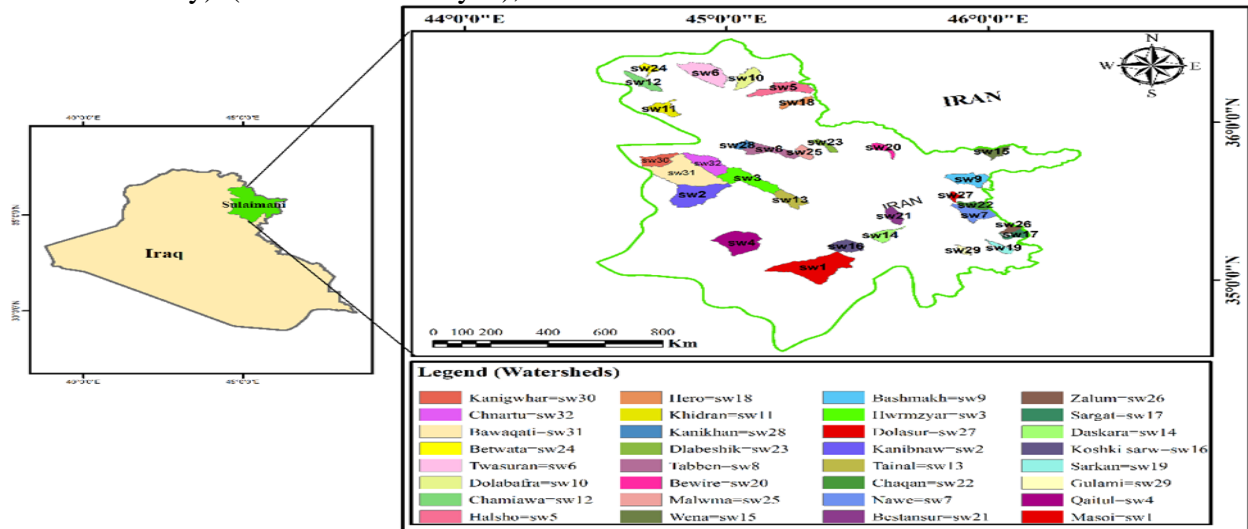


Figure 1. Location of the study area showing the distribution of the selected watersheds over Sulaimani Province

Table 1. Some selected characteristics of the study watersheds

Watershed Code	Local name	Area (km ²)	Perimeter (km)	Maximum elevation(m)	Minimum elevation(m)	&Tc (hour)	#Gravelius Coefficient	L (km)	Nc
SW1	Masoi	314.4	132.9	1810.0	463.0	2.70	2.10	41.3	692
SW 2	Kanibnaw	210.4	100.6	1405.0	556.0	1.67	1.94	22.9	443
SW 3	Hwrmyzar	156.2	97.2	1430.0	766.0	2.00	2.18	27.2	385
SW4	Qaitul	184.6	89.4	1185.0	427.0	1.70	1.84	21.6	393
SW5	Halsho	117.2	89.2	2412.0	522.0	1.76	2.31	27.2	227
SW6	Twasuran	159.9	82.4	2401.0	507.0	1.70	1.82	20.7	360
SW7	Nawe	95.4	73.9	2521.0	523.0	1.36	2.12	16.1	224
SW8	Tabben	87.9	73.0	2604.0	685.0	1.44	2.18	25.8	202
SW9	Bashmakh	97.1	65.0	1907.0	1255.0	1.24	1.85	18.0	236
SW10	Dolabafra	73.6	63.4	1487.0	510.0	1.57	2.07	21.1	126
SW11	Khidran	63.5	61.6	1324.0	503.0	1.15	2.16	21.9	143
SW12	Chamiawa	61.0	60.4	1501.0	529.0	1.59	2.17	22.8	141
SW13	Tainal	71.9	58.2	1337.0	766.0	1.34	1.92	16.8	176
SW14	Daskara	53.8	57.3	1343.0	531.0	1.48	2.19	16.2	105
SW15	Wena	56.8	54.6	2742.0	1229.0	1.11	2.03	14.4	131
SW16	Koshkisarw	76.3	50.6	1807.0	621.0	1.15	1.62	15.2	181
SW17	Sargat	36.2	50.0	2549.0	577.0	0.90	2.33	16.7	77
SW18	Hero	42.3	49.0	2379.0	596.0	1.17	2.11	16.7	93
SW19	Sarkan	31.5	46.7	1343.0	531.0	1.17	2.33	17.7	54
SW20	Bewire	33.9	46.2	2138.0	972.0	1.10	2.22	16.4	74
SW21	Bestansur	50.1	45.9	1345.0	537.0	1.39	1.82	16.6	115
SW22	Chaqaan	42.4	44.6	2194.0	741.0	1.04	1.92	16.9	96
SW23	Dlabeshik	30.1	43.1	2189.0	805.0	1.03	2.20	14.9	73
SW24	Betwata	28.9	40.8	1994.0	629.0	0.86	2.13	11.0	67
SW25	Malwma	39.3	39.5	2401.0	507.0	0.56	1.76	8.6	99
SW26	Zalum	28.3	35.0	2564.0	577.0	0.74	1.84	9.7	62
SW27	Dolasur	19.7	32.5	1599.0	731.0	0.77	2.05	8.7	39
SW28	Kanikhan	29.3	31.9	1600.0	614.0	0.74	1.65	9.1	68
SW29	Gulami	17.7	31.6	898.0	480.0	0.95	2.10	10.5	39
SW 30	Kanigwhar	80.2	48.4	1204.0	410.0	1.45	1.51	21.3	155
SW 31	Bawaqati	315.1	100.8	1443.0	412.0	2.12	1.59	42.8	686
SW 32	Chnartu	119.7	57.2	1443.0	435.0	1.73	1.46	24.2	229
	Minimum	17.7	31.6	898.0	410.0	0.56	1.46	8.6	39.0
	Maximum	315.1	132.9	2742.0	1255.0	2.70	2.33	42.8	692.0
	Average	88.3	61.0	1828.1	623.3	1.33	1.98	19.1	193.5

Tc, Time of concentration; L, Stream length; Nc, Total number of segments

$$\& Tc = 0.119 \left(\frac{L^{0.777}}{S^{0.212}} \right) \text{ Jung (2005)}$$

the Gravelius compactness coefficient, as the most widely accepted shape indices, is defined as the ratio between the basin perimeter and the circumference of a circle with a surface equal to the basin area.

LS is combined slope length and slope steepness factor, C is cropping and management factors (e.g., crops grown, canopy cover, residue cover, surface roughness), and P is erosion control practices (contour tillage and planting, strip-cropping, terracing, subsurface drainage).

R-factor: The R-factor is calculated as long-term mean annual sum of the product of the storm total kinetic energy, E (MJ) and the maximum rain intensity recorded within consecutive 30 min, I_{30} (mm h^{-1}) as shown in Eq. (2):

$$R = \frac{1}{N} \sum_{j=1}^N \left[\sum_{k=1}^{mj} (EI_{30})_k \right]_j \quad (2)$$

where N , years of records; m_j , number of erosive events of a year j . To calculate E and also to obtain I_{30} , the detail rainfall record data are needed for the whole study area. Because of the lack of such data, rainfall erosivity (R) of the rainfall stations across the study area (15 stations) was predicted based on the model proposed by Keya, 2018:

$$R = 1285.16 + 0.183P - 18.475\text{Lat} - 14.431\text{Long} \quad (3)$$

where P is annual rainfall (mm), Lat is Latitude of the station (decimal), and Long is Longitude of the station (decimal). The rainfall data from 15 meteorological stations distributed across the study area for a time span of years 2002-2022 were used in the current study. The R map for Sulaimani province was generated using IDW interpolation scheme.

Soil erodibility: The soil erodibility was estimated using pseudotransfer function according to Renard et al. 1997:

$$K = 0.0035 + 0.038 \exp \left[\frac{-1}{2} \left(\frac{\log Dg + 1.519}{0.7584} \right)^2 \right] \quad (4)$$

$$Dg = \exp \left(0.01 \sum_{i=1}^n f_i \ln m_i \right) \quad (5)$$

where Dg is geometric mean particle diameter of the surface soil layer, f_i is primary particle size fraction (%), m_i is mean of particle size limits (mm), K is soil erodibility ($\text{t h MJ}^{-1} \text{mm}^{-1}$).

The soil data used in this study were two groups. The first group extracted from the previous soil surveys. The second group were

those obtained from soil samples collected from surface (0-15 cm) depth. In overall, 232 soil data were used for K estimation. The K map of each watershed was prepared by IDW tool of GIS considering the soil unit maps, topography, and land use-land cover of the watershed. The map of nonerosive surface was created by using Google Earth and land use/land cover classification map, and include rock outcrop, buildings, and water bodies.

LS factor: Wischmeier and Smith, 1978 defined the L-factor as the ratio of soil lost from a horizontal slope length to the corresponding loss from the slope length of a unit plot (22.13 m). Watershed modeling of soil erosion by RUSLE in GIS is based on algorithms used to calculate LS and the technical procedures described by Moore and Wilson, 1992 presented a simplified equation used to calculate the LS factor as follow:

$$LS = \left(\frac{A_s}{21.13} \right)^{0.4} \left(\frac{\sin \beta}{0.0896} \right)^{1.3} \quad (6)$$

where, A_s is the unit contributing area (m), β is the slope angle in degrees. The Digital Elevation Model (DEM) is used for getting the slope angle and Flow Direction. In the current work, the DEM of the study area with a cell size of 12.5 m was used to estimate LS factor. Slope angle and Flow Direction was determined from DEM. The Flow Direction was used as an input grid to derive the Flow Accumulation that was used to obtain upslope contributing factor.

Crop factor: The Normalized Difference Vegetation Index (NDVI) values were used to derive C factor by the following equation (Van der Knijff et al., 1999):

$$C = \exp \left(-\alpha \frac{NDVI}{\beta - NDVI} \right)^a \quad (7)$$

where, α and β are fitting parameters Van der Knijff et al., 1999 showed that the best value of α and β are 2, and 1 respectively. In this study, the Google Earth Engine (GEE) was used to extract NDVI from Landsat 5 and Landsat 8 satellite images for the periods from 2002 to 2022, with a special resolution of 30 m to create the map of the c-factor. The formula for NDVI takes the following form:

$$NDVI = \frac{NIR - Red}{NIR + Red} \quad (12)$$

where, VIS is the visible (red) spectral band and NIR is the near-infrared spectral band.

P factor: The P-factor is different from the C-factor as it showed the influence of management from the control of runoff, indicating specifically how management practices such as terraces, strip cropping, contour and tillage reduce the speed soil erosion (Renard *et al.*, 1997). In the study area, there was not any support practices therefore the P factor being equal to 1.

Soil erosion risk map

Every soil erosion factor was converted into a grid layer with a cell size of 30×30 meters. Implementation of the RUSLE in a GIS resulted in annual soil loss map for the watersheds. The sum of each pixel value times the pixel area was used to compute the average soil loss. The resultant layer was then divided into five categories of soil erosion risk (Uddin *et al.*, 2016): very low, low, moderate, high, and very high with respective values of <5, 5-10, 10-20, 20-50 and > 50 t ha⁻¹ y⁻¹.

RESULTS AND DISCUSSION

Factors affecting soil erosion

The rainfall erosivity factor (R-factor) was calculated from the average annual rainfall data. The mean rainfall erosivity factor showed a wide range from 73.51 to 632.23 MJ mm ha⁻¹ h⁻¹ for different watersheds (Table 2). In overall, rainfall erosivity show an increasing trend from south west to north east, with a positive correlation with elevation. As

expectation, R also shows spatial variability across each watershed. Figure 2 presents R map, the spatial distribution of the R-factor, in three selected watersheds of the study area. Also, rainfall erosivity show a relationship with elevation in each watershed. The modeling of rainfall erosivity shows that the potential for soil erosion increases with rainfall intensity and duration. The estimated R-value in the study area corresponds with the previous studies in the same and adjacent region. The mean rainfall erosivity of the study area is 146 MJ mm ha⁻¹ h⁻¹ yr⁻¹ which was in consistence with that (156 MJ mm ha⁻¹ yr⁻¹) of Hameed ,2021. The K factor is the soil erodibility factor that is influenced by several factors such as soil texture, organic matter content, structure, permeability, crop, and tillage system. The least detached-resistant soils that produce considerable runoff has the highest values for the K parameter, which measures both the soil's susceptibility to erosion and the rate of runoff. The soil erodibility value is high for all watersheds in high altitudes, the erodibility value is low for all watersheds in low altitudes. Mean K value of the watersheds ranged from 0.0303 to 0.0410 t h MJ⁻¹ mm⁻¹ (Table 2). Clay-rich soils and sandy soils have lower K values but loamy soils have higher K values.

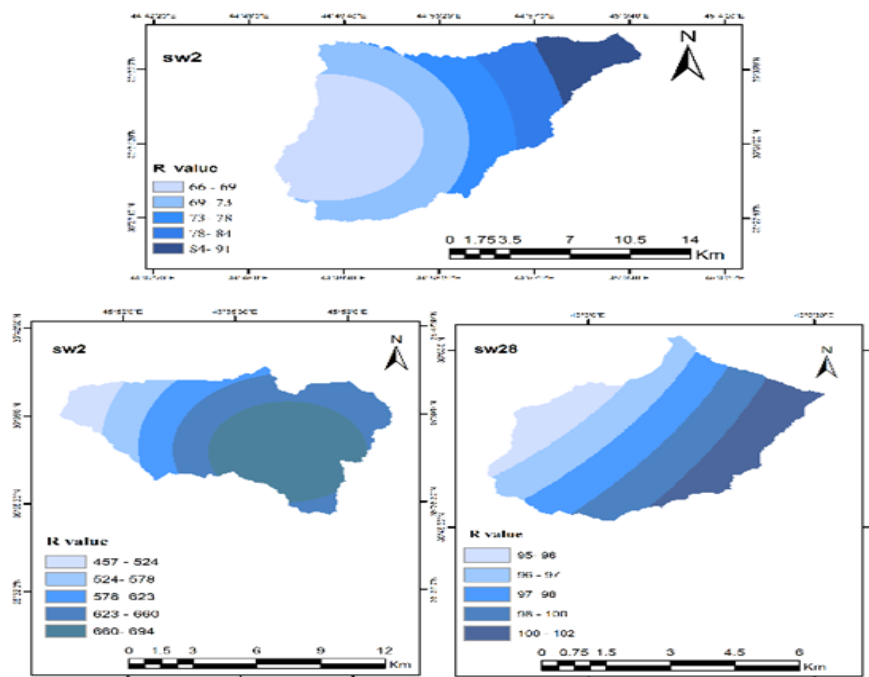


Figure 2. Spatial distribution map of R-factor for some selected watersheds

Table 2. The mean values of the R, K, LS, and C factors for all watersheds

Watershed ID	R (MJ mm ha ⁻¹ h ⁻¹ y ⁻¹)	K (t h MJ ⁻¹ mm ⁻¹)	LS	C
SW1	106.6	0.041	1.72	0.753
SW2	73.5	0.039	1.20	0.734
SW3	96.0	0.035	2.26	0.680
SW4	101.7	0.038	1.69	0.732
SW5	104.4	0.037	5.50	0.654
SW6	110.0	0.030	6.31	0.653
SW7	169.2	0.036	4.05	0.611
SW8	107.3	0.034	6.03	0.589
SW9	632.2	0.039	3.03	0.582
SW10	109.4	0.034	2.79	0.715
SW11	106.2	0.038	3.59	0.645
SW12	109.9	0.038	4.27	0.615
SW13	102.9	0.032	2.33	0.619
SW14	106.5	0.033	1.98	0.655
SW15	366.1	0.039	5.29	0.529
SW16	117.9	0.038	4.49	0.554
SW17	138.1	0.036	7.11	0.610
SW18	107.3	0.041	5.68	0.605
SW19	108.8	0.035	4.68	0.633
SW20	140.0	0.041	5.98	0.574
SW21	86.2	0.033	1.77	0.661
SW22	266.4	0.038	7.42	0.593
SW23	123.2	0.039	6.96	0.570
SW24	110.5	0.041	7.05	0.602
SW25	116.7	0.037	6.32	0.460
SW26	147.7	0.035	9.32	0.589
SW27	369.5	0.041	6.78	0.604
SW28	98.3	0.034	3.85	0.594
SW29	104.5	0.040	2.35	0.615
SW30	96.6	0.034	2.08	0.739
SW31	85.9	0.036	1.89	0.743
SW32	97.5	0.038	2.95	0.680
Minimum	73.5	0.030	1.20	0.460
Maximum	632.2	0.041	9.32	0.753
Average	147.4	0.037	4.34	0.631

The lowest values of the K-factor were found in alluvial soils, and the highest values of the K-factor were found in the area contained thin soils on steep slopes. While there were not considerable differences among watershed's mean K value, K parameter showed spatial variation in each watershed (Fig. 3). The LS factor was calculated to quantify the slope lengths and gradient's impact on soil erosion risk. The mean values of LS-factor for all studied watersheds are presented in Table 2. The mean LS factor ranged from 1.20 to 9.32. This means that the soil erosion risk induced by topography is 6.7 higher for the watershed with highest risk (Zalum) than the watershed with the lowest risk (Kanibnaw). Generally,

topography-induced soil erosion risk increased from south west to north and north east of Sulaimani province. Obviously, the spatial variation of LS-factor is very high in each watershed (Fig. 4) The lowest LS values are located in the down-slope lands, reflecting the slope effect on the LS outcomes. The LS values were higher in the mountainous area of any watersheds in the study area. The map showed that LS values are directly related to surface relief. The effect of slope's length and gradient are quantified by LS factor, the steeper the slope and the longer the slope length, the higher the runoff velocities and rates, and thus, the higher soil erosion risk. The SL value is high for all watersheds in high

altitudes, the LS value is low for all watersheds in low altitudes. The effect of slope's length and gradient are quantified by LS factor, the steeper the slope and the longer

the slope length, the higher the runoff velocities and rates, and thus, the higher soil erosion risk.

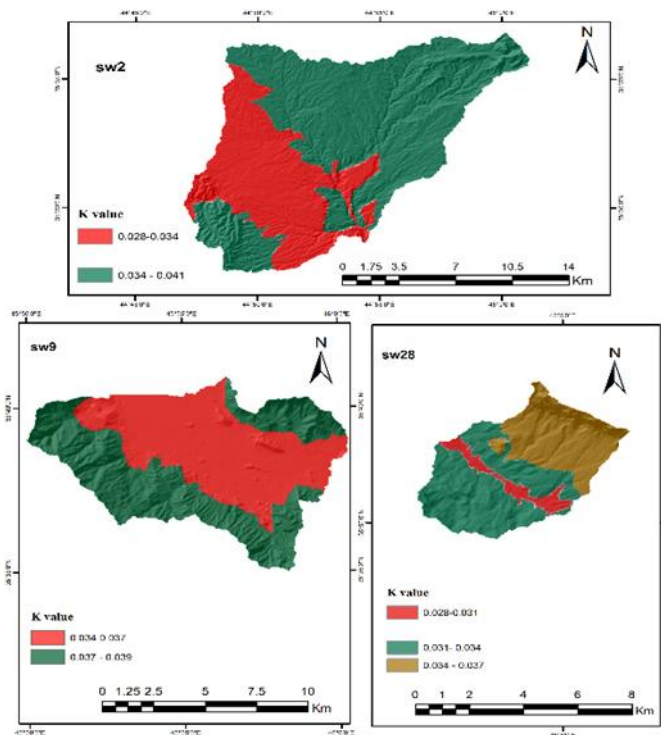


Figure 3. Spatial distribution map of K-factor for three selected watersheds

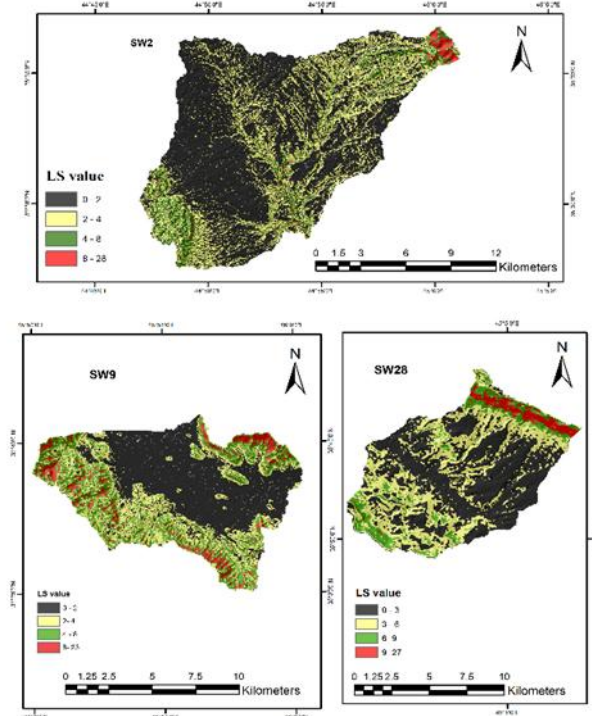


Figure 4. Spatial distribution map of LS-factor values for three selected watersheds

The C factor values ranged from 0.4596 to 0.7533 in average for the 32 watersheds (Table 2) showing the poor vegetation cover of the

watersheds in general. In spite of this general view, there are area with reasonable vegetation cover resulting in low C factor ($C < 0.1$) in one

side, and the area of bare soils ($C \approx 1$) in another side in each watershed (Fig. 5). Typically, the areas with low C values are covered with dense forest or orchards, while the area with the highest C values have bare soils, residential area and rocks. The average C-factor value for all watersheds is higher than 0.46, which indicates poor cover vegetation.

Spatial distribution of soil erosion across the study watersheds: The components of the RUSLE model in the study area were represented as raster layers in the GIS environment, and they were multiplied to provide the erosion risk map for each watershed. Fig. 6 shows the geographical distribution of soil erosion risk (soil loss) in three selected watersheds. It is clear that, the soil erosion risk has a high topographically-related spatial variability across each watershed. As discussed in Materials and Methods section, the soil erosion risk was categorized in five classes of very low, low, moderate, high, and very high. Also, the area-weighted mean soil erosion risk was calculated for each watershed. The results are summarized in Table 3. The average soil erosion risk ranged from 2.12 ton ha⁻¹ y⁻¹ (for Kanibnaw watershed located in the west of Sulaimani province) to 62.05 ton ha⁻¹ y⁻¹ (for Dolasur watershed located in the east of the

province). The results of extend of soil erosion risk classes across the watershed show that watersheds located in the east of Sulaimani province have soil loss erosion risk more than the watersheds in the west, illustrated in Table 3. Generally, 9 among 32 watersheds exhibited very low risk of soil erosion (< 5 ton ha⁻¹ y⁻¹), and one watershed showed very high soil erosion risk (>50 ton ha⁻¹ y⁻¹) in average. All watersheds had the regions with high (between 2 to 20 percent of watersheds area) and very high (between 0.5 to 7 percent of watersheds area) soil erosion risks (Table 3). Results show that the average annual soil loss for all watersheds has a different value from 2.12 to 62.05 t ha⁻¹ y⁻¹. Other studies have calculated historical (Mutekanga *et al.*, 2010.) or future (Prasuhn *et al.*, 2013) soil erosion risk considering the changes in land use and land cover. To confirm the long-term average soil loss, long-term measurement series from actually cultivated plots are also necessary (Prasuhn *et al.*, 2013). Since there were no data to validate soil loss predicts across the region, only a qualitative visual survey was used to validate the obtained map. Particularly for the regions with potentially low and extremely high erosion risks, there was a good geographic

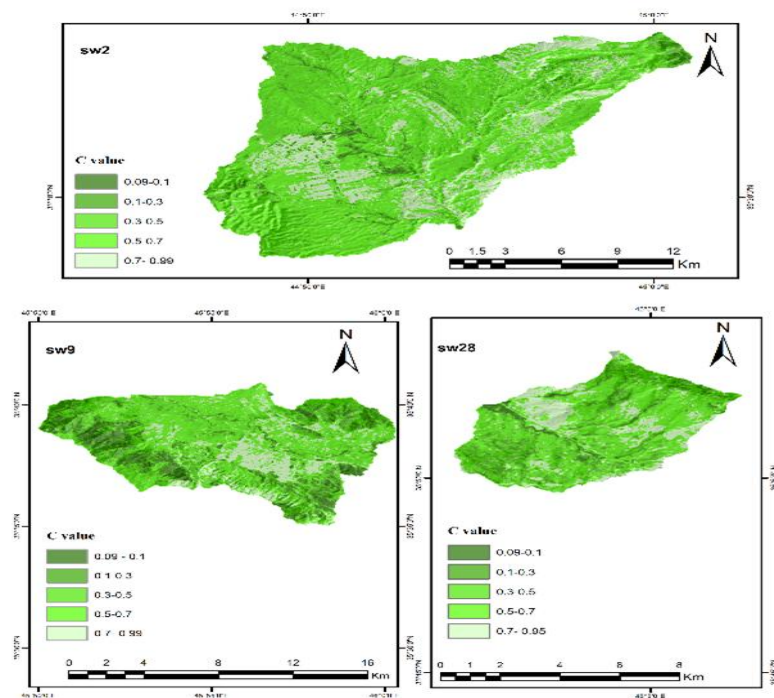


Figure 5. Spatial distribution map of C-factor values for three selected watersheds

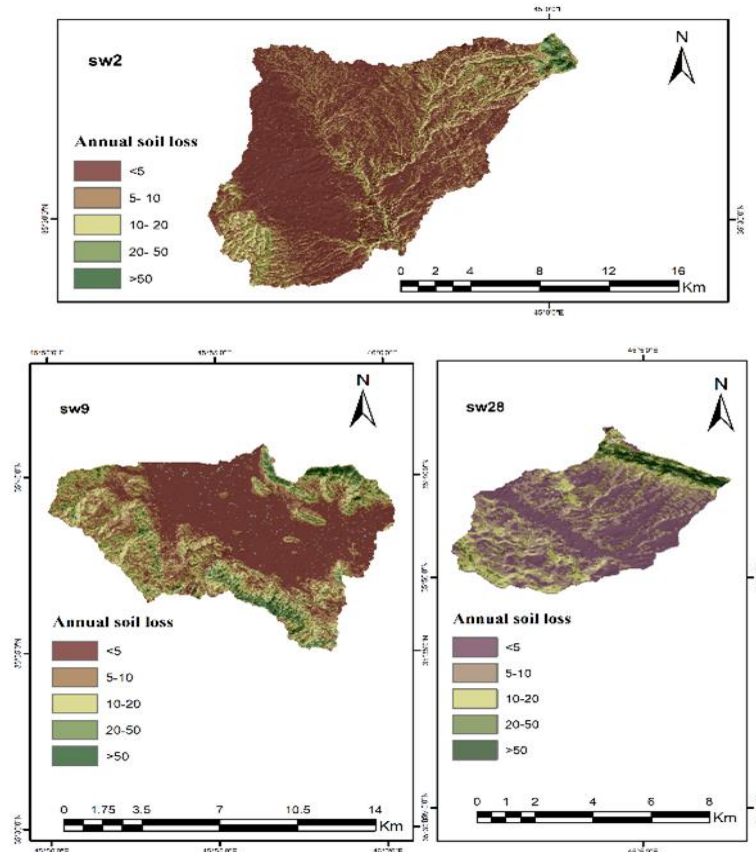


Figure 6. Spatial distribution map of average annual soil loss for three selected watersheds

agreement between the mapped soil loss and the field observations of soil erosion features. While with quite different spatial extent, soil erosion risk ranged from zero (for non-erodible area including rock outcrops, roads, residential region) to $> 100 \text{ t ha}^{-1} \text{ y}^{-1}$ in all watersheds. This is in accordance with the reports from different world regions. Angima *et al.*, 2003 predicted the average soil loss in an agricultural catchment in central Kenyan highlands to be $134 \text{ t ha}^{-1} \text{ y}^{-1}$ for segments with LS factors between 0 and 10, $420 \text{ t ha}^{-1} \text{ y}^{-1}$ for segments with LS-factors between 10 and 20, and $549 \text{ t ha}^{-1} \text{ y}^{-1}$ for slopes with LS-factors between 20 and 30. A similar methodology was used by Prasuhn *et al.* (Prasuhn *et al.*, 2013) to produce the soil erosion risk map for Switzerland. Gelagay and Minale, 2016 found that the average soil erosion rate in the Blue Nile basin's Koga watershed was 47.4 t ha^{-1} per year. According to research by Fallah *et al.*, 2023 soil erosion ranged from 0 to higher than $100 \text{ t ha}^{-1} \text{ y}^{-1}$ in Navroud watershed, North of Iran. In this research (Eltaif and Gharaibeh, 2022) outcrops and very dense natural forests at gentle slopes exhibited

almost zero erosion, on the other hand, bare soils and deforested area at steep slopes showed severe soil erosion. Abate, 2011 which reported an erosion rate of more than $80 \text{ t ha}^{-1} \text{ y}^{-1}$ on steep slope sections in the Borena watershed. It is not feasible to undertake soil conservation measures across the entire watershed at once due to resource constraints. It is crucial to prioritize intervention areas according to the severity and risks of soil erosion. Therefore, as also suggested by Abate, 2011, and Gizachew, 2015 for their respective study sites, implementing soil conservation measures based on the given priority is a better option. These findings may provide guidance in identifying and targeting the watersheds in Sulaimani province, and rangelands and croplands in each watershed at greatest potential risk of soil erosion for additional monitoring, mitigation and management practices. In the current study, the region/area with high rainfalls, the dominance of loamy soil, elevated terrains/plateau edges with a steep side slope, and significant farming activity were all associated with high soil loss rates. There is

little doubt that the basin's upstream regions are places with a significant potential for soil erosion. The findings of the present study could therefore be used to inform decision-making for better soil management and land conservation. The required steps should be taken by public authorities to lessen the impact of these influencing characteristics. Zones with

flat plains and low slopes, where soil erosion by water is not a prominent characteristic, are where the low and mild erosion risk zones are located. The other regions, on the other hand, are situated in a basin with a high and extreme risk of erosion, where the mountainous topography, steep slopes, and improper agricultural methods exacerbate soil erosion.

Table 3. The average predicted soil loss (A) and the area (%) of each soil erosion risk class for all watersheds

Watershed ID	Average soil erosion risk		Soil erosion risk class				
	A (ton ha ⁻¹ y ⁻¹)	class	Very low (<5)	Low (5-10)	Moderate (10-20)	high (20-50)	Very high (>50)
SW1	3.85	Very low	46.23	37.59	12.19	3.12	0.86
SW2	2.12	Very low	58.34	28.81	10.15	2.11	0.58
SW3	3.13	Very low	69.32	11.78	10.48	6.36	2.06
SW4	4.10	Very low	48.77	36.96	10.80	2.55	0.92
SW5	12.19	Moderate	40.69	25.32	19.17	10.87	3.95
SW6	16.00	Moderate	36.10	23.93	24.63	12.28	3.06
SW7	17.36	Moderate	47.92	20.22	17.85	10.81	3.19
SW8	9.92	Low	47.92	20.22	17.85	10.81	3.19
SW9	36.77	High	47.92	20.22	17.85	10.81	3.19
SW10	7.49	Low	47.92	20.22	17.85	10.81	3.19
SW11	8.87	Low	47.92	20.22	17.85	10.81	3.19
SW12	9.95	Low	34.77	23.57	19.47	14.99	7.20
SW13	4.29	Very low	55.74	18.34	14.41	8.60	2.90
SW14	4.25	Very low	53.31	23.01	13.30	7.90	2.48
SW15	31.76	High	23.51	33.38	26.34	12.96	3.81
SW16	8.57	Low	41.14	32.30	18.14	6.49	1.93
SW17	21.64	High	30.09	25.40	23.65	15.71	5.14
SW18	14.89	Moderate	25.36	33.80	25.74	12.70	2.40
SW19	11.84	Moderate	35.70	21.24	21.97	15.91	5.18
SW20	19.00	Moderate	21.54	31.93	26.13	15.65	4.76
SW21	3.92	Very low	62.78	14.21	11.13	8.34	3.53
SW22	40.27	High	22.98	26.13	27.75	18.14	5.00
SW23	15.70	Moderate	20.52	29.78	27.58	16.55	5.56
SW24	18.64	Moderate	27.85	31.67	24.90	12.25	3.33
SW25	12.18	Moderate	34.94	30.19	20.72	10.85	3.30
SW26	27.40	High	23.32	25.63	25.73	19.43	5.89
SW27	62.05	Very High	18.50	27.34	27.75	19.46	6.94
SW28	7.63	Low	41.34	34.27	15.69	5.88	2.81
SW29	6.12	Low	26.20	30.94	24.86	14.23	3.77
SW30	4.22	Very low	42.61	35.02	15.72	6.13	0.52
SW31	3.04	Very low	54.54	31.66	9.95	3.05	0.80
SW32	6.62	Low	37.73	26.19	18.65	12.47	4.97
Minimum	2.12		18.50	11.78	9.95	2.11	0.52
Maximum	62.05		69.32	37.59	27.75	19.46	7.20
Average	14.24		39.80	26.61	19.26	10.91	3.43

CONCLUSIONS

The RUSLE and GIS framework were used to map soil erosion risk in Sulaimani province, northern Iraq. Factors such as rainfall erosivity, soil erodibility, slope length and steepness, vegetation cover, and conservation support practice were calculated for 32 watersheds. The mean soil loss value was calculated for all watersheds, with the lowest value being 2.12 t ha⁻¹ y⁻¹ and the highest being 62.05 t ha⁻¹ y⁻¹.

CONFLICT OF INTEREST

The authors declare that they have no conflicts of interest.

DECLARATION OF FUND

The authors declare that they have not received a fund.

REFERENCES

Abate, S. 2011. Estimating soil loss rates for soil conservation planning in the Borena woreda of South Wollo highlands, Ethiopia. *J. Sustain. Dev. Afr.* 13(3), 87-106.

<https://www.ajol.info/index.php/ejbe>

AbdelRahman, M.A. 2023. An overview of land degradation, desertification and sustainable land management using GIS and remote sensing applications. *Rendiconti Lincei. Scienze Fisiche e Naturali*, 34, (No.) 767–808.

<https://doi.org/10.1007/s12210-023-01155-3>

Angima, S., D. Stott, M. O’neill, C. Ong and G. Weesies. 2003. Soil erosion prediction using RUSLE for central Kenyan highland conditions. *Agriculture, Ecosystems & Environment* 97, 295-308.

[https://doi.org/10.1016/S0167-8809\(03\)00011-2](https://doi.org/10.1016/S0167-8809(03)00011-2)

Asadi, H., M. Honarmand, M. Vazifedoust and A. Moussavi. 2017. Assessment of changes in soil erosion risk using RUSLE in Navrood Watershed, Iran. *Journal of Agricultural Science and Technology* 19, 231-244.

<http://jast.modares.ac.ir/article-23-7096-en.html>

Mehdizade, B., H. Asadi, M. Shabanpour, and H. Ghadiri. 2013. The impact of erosion and tillage on the productivity and quality of selected semiarid soils of Iran. *International Agrophysics*, 27, 291-297. doi: 10.2478/v10247-012-0097-4

Eltaif, N.I. and M.A. Gharaibeh. 2022. Soil erosion catastrophe in Iraq-preview, causes and study cases. In: Al-Quraishi, A.M.F., Mustafa, Y.T., Negm, A.M. (eds) *Environmental Degradation in Asia*. Earth and Environmental Sciences Library. Springer, Cham. 179-207. http://dx.doi.org/10.1007/978-3-031-12112-8_9

Fallah, M., H. Bahrami, and H. Asadi 2023. Assessment of soil erosion risk using RUSLE model, SATEEC system, remote sensing, and GIS techniques: a case study of Navroud watershed. *Environ. Earth Sci.* 82, 398.

<https://doi.org/10.1007/s12665-023-11053-4>

Gelagay, H.S. and A.S. Minale. 2016. Soil loss estimation using GIS and Remote sensing techniques: A case of Koga watershed, Northwestern Ethiopia. *International Soil and Water Conservation Research* 4, 126-136.

<https://doi.org/10.1016/j.iswcr.2016.01.002>

Gizachew, A. 2015. A geographic information system based soil loss and sediment estimation in Zingin watershed for conservation planning, highlands of Ethiopia. *World Appl. Sci. J.* 33(1): 69–79.

DOI:10.11648/j.ijsts.20150301.14

Jensen, J.R. 2009. Remote sensing of the environment: An earth resource perspective 2/e. Pearson Education India. Book.

Hameed, H.M. 2021. Soil erosion assessment within the Erbil watershed using geoinformatics technology. *Halabja University Journal* 6, 311-329.

<http://dx.doi.org/10.32410/huj-10375>

Keya, D. 2018. Integration of GIS with USLE in assessing soil loss from Alibag catchment, Iraqi Kurdistan Region. *Polytechnic Journal* 8, 269-281.

DOI: <https://doi.org/10.25156/ptj.2018.8.1.66>

Molnárová, K.J., P. Sklenička, I.C. Bohnet, F. Lowther-Harris, A. van den Brink, S.M. Moghaddam, V. Fanta, V. Zástěra and H. Azadi. 2023. Impacts of land consolidation on land degradation: A systematic review. *Journal of Environmental Management* 329, 117026.

Moore, I.D. and J.P. Wilson. 1992. Length-slope factors for the Revised Universal Soil Loss Equation: Simplified method of estimation. *Journal of soil and water conservation* 47, 423-428.

<http://www.swcs.org/>

- Mutekanga, F.P., S.M. Visser and L. Stroosnijder. 2010. A tool for rapid assessment of erosion risk to support decision-making and policy development at the Ngenge watershed in Uganda. *Geoderma* 160, 165-174. <https://doi.org/10.1016/j.geoderma.2010.09.011>
- Prasuhn, V., H. Liniger, S. Gisler, K. Herweg, A. Candinas and J.-P. Clément. 2013. A high-resolution soil erosion risk map of Switzerland as strategic policy support system. *Land Use Policy* 32, 281-291. <https://doi.org/10.1016/j.landusepol.2012.11.006>
- Räsänen, T.A., M. Tähtikarhu, J. Uusi-Kämpä, S. Piirainen and E. Turtola. 2023. Evaluation of RUSLE and spatial assessment of agricultural soil erosion in Finland. *Geoderma Regional* 32, e 00610. <http://dx.doi.org/10.1016/j.geodrs.2023.e00610>
- Renard, K., Foster, G., Weesies, G., Mccool, D., Yoder, D., 1997. Predicting soil erosion by water: a guide to conservation planning with the Revised Universal Soil Loss Equation (RUSLE), US Department of Agriculture, Agricultural Research Service. Book
- Singh, M.C., K. Sur, N. Al-Ansari, P.K. Arya, V.K. Verma, A. Malik. 2023. GIS integrated RUSLE model-based soil loss estimation and watershed prioritization for land and water conservation aspects. *Frontiers in Environmental Science* 11, 1136243. <http://dx.doi.org/10.3389/fenvs.2023.1136243>
- Sreedevi, P., P. Sreekanth, H. Khan and S. Ahmed. 2013. Drainage morphometry and its influence on hydrology in an semi arid region: using SRTM data and GIS. *Environmental Earth Sciences* 70, 839-848. <https://doi.org/10.1007/s12665-012-2172-3>
- Tetzlaff, D., S. Carey and C. Soulsby. 2013. Cthments in the future North: interdisciplinary science for sustainable management in the 21st Century. north-Watch Workshop, Potsdam, Germany, 21-25 May 2012. *Hydrological Processes* 27, 635-774.
- Uddin, K., M. Murthy, S.M. Wahid and M.A. Matin. 2016. Estimation of soil erosion dynamics in the Koshi basin using GIS and remote sensing to assess priority areas for conservation. *PloS one* 11, e0150494. <https://doi.org/10.1371/journal.pone.0150494>
- Van der Knijff, J., R. Jones and L. Montanarella. 1999. Soil erosion risk assessment

تقييم مخاطر تعرية التربة باستعمال المعادلة العامة (RUSLE) في احواض تغذية مختارة في محافظة

السليمانية، العراق

ستار صديق عبد الله¹، حسين أسدي²، خالد طيب محمد البرزنجي³، طارق حمه كريم⁴، علي أكبر نزاري السمانى⁵*

²كلية الموارد الطبيعية، جامعة طهران، كرج، إيران

³قسم الموارد الطبيعية، كلية علوم الهندسة الزراعية، جامعة السليمانية، السليمانية، العراق

⁴قسم هندسة المساحة والجيوماتكس، كلية الهندسة، جامعة تيشك الدولية، أربيل، العراق

⁵كلية الموارد الطبيعية، جامعة طهران، كرج، إيران

المستخلص

ان الهدف من هذه الدراسة هو تقييم خطر تآكل التربة في 32 حوض نهري ضمن محافظة السليمانية، كردستان/العراق ، استناداً إلى بيانات المعادلة العامة (RUSLE) لمفقودات التربة ونظم المعلومات الجغرافية وبيانات RS . استخدم بيانات معدل الأمطار السنوية لتوليد عامل تآكل جريان الأمطار باستخدام المعادلة التي تم تطويرها مسبقاً للمنطقة. تم تقدير عامل تآكل التربة باستخدام بيانات التوزيع الحجمي لمفصولات التربة. تم إنشاء العامل الطبوغرافي باستخدام نموذج الارتفاع الرقمي من مرئية فضائية Sentinel-2 . كما وحدد عامل إدارة الغطاء باستخدام Google Earth Engine مع Landsat7 وLandsat8. تبين من النتائج بأن عوامل تآكل التربة والغطاء النباتي لم تظهر تبايناً مكانياً كبيراً في جميع أنحاء منطقة الدراسة، فقد أظهرت تآكل التساقط المطري اتجاهًا متزايداً من الجنوب الغربي إلى الشمال الشرقي من المنطقة، وتراوح من 73 إلى 632 ميغا جول ملم هكتار⁻¹ ساعة⁻¹. أظهرت النتائج أن متوسط فقدان التربة السنوي لاحواض التغذية المختلفة يتراوح من 2.12 إلى 62.05 طن هكتار⁻¹ سنة⁻¹. كما أشارت النتائج إلى أن العوامل الرئيسية التي تؤثر على تآكل التربة في محافظة السليمانية هي كثافة التساقط المطري والتضاريس الوعرة والمنحدرات الشديدة وتناثر النباتات.

الكلمات المفتاحية: قابلية التربة للتعرية، تحسس نائي، صيانة سليمانية، غطاء نباتي.